Tikrit Journal of Engineering Sciences (2025); 32(Sp1): 2580
DOI: http://doi.org/10.25130/tjes.sp1.2025.5

IRAQI Academic Scientific Journals

ISSN: 1813-162X (Print); 2312-7589 (Online)
Tikrit Journal of Engineering Sciences
available online at: http://www.tj-es.com

TJES Tikrit Journal of Engineering Sciences

Photovoltaic Stand-Alone Systems Using an Artificial Neural Network-Based Intelligent Control System

Yaseen Al-Husban [a], Takialddin Al Smadi [*b], Suprava Ranjan Laha [c], Khalid Al Smadi [d]

a Department of Communications and Electronics Engineering, Isra University, Jordan.
b Member IEEE, Faculty of Engineering, Jerash University, Jordan.
c Department of Computer Science Engineering, ITER- Siksha 'O' Anusandhan Deemed to be University, Bhubaneswar, Odisha, India.
d Business Intelligence Department, Business School, Jadara University, Irbid, Jordan.

Keywords:
Artificial Neural Networks; Maximum Power Point Tracking; Photovoltaic Systems; PID Control; Renewable Energy Optimization.

Highlights:

- *Hybrid ANN architecture: tanh & ReLU in 6-3 layers for fast MPPT.*
- *Outperforms P&O (95.1%), INC (96.0%), ANN (98.1%): 99.2% accuracy.*
- *ANN-PID minimizes voltage ripple to <1.5% during mode transitions.*
- *Efficient training: 1.73e−5 MSE in 200 epochs with Levenberg-Marquardt.*

ARTICLE INFO

Article history:

Received	29 Mar. 2025
Received in revised form	06 May. 2025
Accepted	08 July 2025
Final Proofreading	09 Aug. 2025
Available online	10 Sep. 2025

Citation: Al-Husban Y, Al Smadi T, Laha SR, Al Smadi K. **Photovoltaic Stand-Alone Systems Using an Artificial Neural Network-Based Intelligent Control System**. *Tikrit Journal of Engineering Sciences* 2025; **32**(Sp1): 2580. http://doi.org/10.25130/tjes.sp1.2025.5

*Corresponding author:
Takialddin Al Smadi
Member IEEE, Faculty of Engineering, Jerash University, Jordan.

Abstract: This study introduces an adaptive artificial neural network (ANN)-based control system to enhance the efficiency of stand-alone photovoltaic (PV) systems under dynamic environmental conditions. Traditional maximum power point tracking (MPPT) methods, such as perturb and observe (P&O) and incremental conductance (INC), are hindered by slow convergence and oscillations. The proposed approach utilizes a hybrid ANN architecture with hyperbolic tangent (tanh) and rectified linear unit (ReLU) activation functions in a 6-3 neuron hidden layer structure, enabling real-time prediction of the optimal voltage (V_mpp). Integrated with a PID-controlled DC-DC boost converter, the system seamlessly transitions between the solar harvesting, battery charging, and load supply modes. Trained on 10,000 environmental samples (irradiance: 150–1000 W/m² and temperature: 25–50°C) using the Levenberg-Marquardt algorithm, the ANN achieved 99.2% tracking accuracy with a mean squared error (MSE) of 1.73×10^{-5} in 200 epochs. MATLAB/Simulink simulations demonstrated superior performance, surpassing P&O by 4.1% and INC by 3.2%, while maintaining a voltage ripple below 1.5%. Key innovations include the hybrid ANN design that mitigates saturation effects, adaptive PID tuning for minimal oscillations, and a three-mode converter that ensures a stable 24 V load voltage during irradiance fluctuations. This work underscores the potential of machine learning in advancing renewable energy systems, offering a computationally efficient and hardware-ready solution for off-grid applications with enhanced reliability and precision.

إدارة الطاقة باستخدام أنظمة الطاقة الشمسية الهجينة: دراسة كفاءتها في إنتاج الكهرباء والحرارة

ياسين الحسبان[١]، تقي الدين الصمادي[٢]، سوبرافا رانجان لها[٣]، خالد الصمادي[٤]

[١] قسم هندسة الاتصالات والإلكترونيات/ جامعة الإسراء/ الأردن.

[٢] عضو في معهد مهندسي الكهرباء والإلكترونيات (IEEE)/ كلية الهندسة/ جامعة جرش/ الأردن.

[٣] قسم هندسة علوم الحاسوب/ جامعة إيتر- سيكشا "أو" أنوساندان ديمد/ بوبانسوار/ أوديشا - الهند.

[٤] قسم ذكاء الأعمال/ كلية إدارة الأعمال/ جامعة جدارا/ إربد - الأردن.

الخلاصة

أصبحت أنظمة الطاقة الشمسية الكهروضوئية (PV) تحظى بشعبية متزايدة بسبب تغير المناخ والحاجة إلى تقليل انبعاثات الكربون. تتحكم المحولات الثابتة ووحدات التحكم التناسبية التكاميلية في القوى النشطة والتفاعلية. تحسن بطاريات تخزين الطاقة جودة الطاقة من خلال تخزين التيار والجهد. درس الباحثون نظامًا هجينًا للطاقة الشمسية الكهروضوئية/الحرارية (PVT) يقوم بتخزين الطاقة الحرارية ويستخدم سائلين لنقل الحرارة. أشارت الاختبارات الخارجية إلى أن المجمع الهجين للتبريد يخفض درجة حرارة اللوحة بشكل كبير. في فبراير، وصلت الكفاءة الكهربائية القصوى إلى ١٥,٧١٪، وهو ما يزيد بنسبة ٢٢٪ عن كفاءة اللوحة العادية. كان النظام أيضًا بكفاءة ٦٩,٢٥٪ في استعادة الحرارة و٨٤,٤٠٪ في استعادة الحرارة الكلية عندما تم الحفاظ على معدلات تدفق الهواء والماء كما هي. يمكن لأنظمة PVT تلبية ٦٠٪ من احتياجات التدفئة و١٠٠٪ من احتياجات التبريد في المنازل المنتشرة عبر أربعة مواقع. هذه الأنظمة أقل تكلفة بنسبة ٣٠٪–٤٠٪ مقارنة بأنظمة الطاقة الشمسية فقط. يتم اقتراح عوامل دراسية لتطوير نماذج التنبؤ بالطاقة الشمسية. يمكن أن توجه نتائج هذا التقييم الأبحاث الحالية حول تصميم وتنفيذ أنظمة إدارة الطاقة المتكاملة وتأثيرها على أنظمة الطاقة.تُبرز النتائج أنظمة PVT كبديل مستدام وفعال من حيث التكلفة للمناطق ذات الإمكانات الشمسية العالية، بينما يمهد دمج الذكاء الاصطناعي الطريق لأنظمة طاقة أكثر ذكاءً وتكيفاً. تشمل اتجاهات البحث المستقبلية التحقق عبر المناطق، وتطوير المواد المتقدمة، وإطارات السياسات لدعم النشر على نطاق واسع. يساهم هذا العمل في الانتقال العالمي نحو مرونة الطاقة المتجددة من خلال معالجة التحديات التقنية والاقتصادية في تقنيات الطاقة الشمسية الهجينة.

الكلمات الدالة: إدارة الطاقة، الطاقة الشمسية، النظام الهجين، الكهروضوئي/الحراري (PVT).

1.INTRODUCTION

Photovoltaic systems are pivotal in transitioning to sustainable energy, yet their nonlinear power-voltage characteristics and sensitivity to environmental variability hinder efficiency [1]. While conventional MPPT algorithms, such as P&O and INC, are widely adopted, their reliance on heuristic tuning and suboptimal dynamic response limits performance. Recent advancements in machine learning, particularly ANNs, offer robust solutions for real-time MPPT by modeling complex nonlinear relationships. Although significant achievements have been made in MPPT for stand-alone PV systems, the main limitations remain when considering them collaboratively. Classical algorithms such as P&O and INC are based on static heuristics, resulting in substantial oscillations and sluggish performance under variations in irradiance or temperature. Conventional ANN-based trackers in the literature only adopt a single kind of activation function that saturates or requires over-parameterized training to obtain an acceptable accuracy, and their outputs are usually not synchronized with the real-time converter modulation, which may result in ripple/instability during mode transitions. At the same time, the conventional designs of the converter/topology typically deal with solar harvesting, battery charging, and load supply as separate or weakly correlated modes, making it difficult to achieve a seamless transition or output regulation under environmental fluctuations. To the best of the authors' knowledge, no previous work has incorporated (1) a hybrid activation ANN to circumvent saturation and accelerate convergence; (2) real-time adaptive control that combines an ANN prediction with converter modulation for ripple minimization during transients; and (3) 3-mode energy management scheme that designs such a topology provides an untangled PEF among harvesting, storage, and load. The present study addresses these challenges by integrating an ANN-based control system with adaptive PID tuning. A two-hidden-layer feed-forward ANN for the real-time tracking of photovoltaic arrays' maximum power point (MPPT) under varying irradiance and temperature has been proposed and confirmed. In contrast with the classical perturb-and-observe or incremental-conductance algorithms, which have a built-in oscillatory behavior around the MPP and do not easily learn in fast-varying situations, the ANN learns directly the nonlinear function that maps the environmental and electrical inputs to the optimal operating voltage. The paper makes the following contributions:

1- A 4–6–3–1 architecture of an ANN consisting of tanh activations of the hidden layer and a ReLU output to avoid saturation issues and improve the gradient flow.
2- The proposed method decreases the steady-state oscillations compared to conventional schemes, reaching a mean MPP-tracking accuracy of 99.2 % and a tight ±0.4 % 95 % confidence interval through extensive 10-fold cross-validation on 10000 samples.
3- Utilizing Levenberg–Marquardt training enabled the ANN to achieve convergence in under 200 epochs, and the model can respond within milliseconds to step changes in irradiance faster than what can be achieved with hill-climbing strategies commonly used for this type of control.

4- The ANN output is integrated with a PID-controlled DC–DC converter to achieve <1.5 % voltage ripple during mode transitions, and the performance is experimentally validated under realistic outdoor conditions.

Overall, these improvements show that a properly configured and trained ANN can provide both increased efficiency and an even more responsive system than what conventional MPPT methods have already allowed for, thereby opening the door for new, more intelligent ways of managing equivalent-μ-generation. The use of photovoltaic (PV) technology in power generation from renewable energy sources is a feasible alternative due to its economic feasibility and proper sizing of components. PV generation systems are particularly attractive for remote and isolated locations and small-scale applications, such as PV freezers and water-pumping systems. The decrease in the cost of PV modules and the rise in conventional petrochemical fuel prices have increased the adoption of PV-generations [3]. The photovoltaic effect in power generation offers numerous advantages, including reduced pollutant emissions, silent operation, prolonged lifespan, and minimal maintenance requirements. Solar energy also exhibits characteristics, such as abundance, zero cost, and environmental friendliness [2-5]. Modeling the photovoltaic power systems is crucial before sizing, identification, or simulation efforts. A stand-alone setup usually includes a solar panel system, a battery for storing energy, devices that change direct current to alternating current, users that need both AC and DC power, and a system to manage the power; the solar generator can have several solar arrays, each made up of multiple panels and solar cells. The battery bank stores the surplus energy created by the PV modules when the electricity they provide exceeds the load's requirement. When the PV supply fails to meet the load's demands, it discharges this energy. The power conditioning system acts as an intermediary within the system, providing protective measures and regulatory functionalities. Analytical or numerical approaches have established numerous models to represent and simulate different components in independent photovoltaic power systems. The power cascade, consisting of a DC/DC converter and an inverter, plays a crucial role in most solar power plants. Transformers with a minimum efficiency rating of 90% are essential for optimal energy collection from the solar battery while maintaining the power plant's [6]. The performance of solar cells is significantly influenced by light and temperature, and the optimal algorithm of maximum power point tracking (MPPT) is essential for maximum energy extraction from a solar battery. Optical time division multiplexing (OTDM) uses specialized controllers to optimize the work point of the light module. To achieve the maximum electricity from the solar cells, it must consistently regulate the battery voltage at its ideal level. Despite advancements in solar cell technology, contemporary and efficient management of photovoltaic installations requires addressing design concerns and control systems to enhance energy efficiency significantly [7-8]. The management algorithm must determine the optimal source for meeting the energy requirements of the PV installation, which may include using a locally situated installation, relying on batteries, or borrowing energy from a neighboring installation. Figure 1 represents the use of two photovoltaic (PV) stations with a dump load. Each photovoltaic (PV) station transitions to providing power to its designated load once it receives adequate energy. During a power outage, both the power stations and batteries play a crucial role in assisting. The present study employed the designations K1, K2, K12, K21, K1D, and K2D to identify the IGBT switches. Figure 1 shows dual stand-alone photovoltaic systems with dump loads. Artificial neural networks (ANNs) have been widely used in numerous complex fields. These devices can manage the voltage-dependent electrical network, along with the properties of the current and heat in the cables [9-11]. The FLC demonstrated exceptional precision in regulating a bidirectional total power charger, facilitating both vehicle charging and energy supply to the grid (V2G) [12]. The FLC autonomously calculates the cooking duration for the microwave oven according to the quantity and kind of food. It is used in hybrid power systems, encompassing renewable energy sources both with and without storage [9-10]. Solar arrays, or solar panels and cells, turn sunlight into electricity via the photovoltaic effect. These arrays comprise several interconnected solar cells fabricated from semiconductor materials, including silicon. When sunlight impinges upon the solar cells, the photons within the light energize the electrons in the semiconductor, resulting in the generation of electricity. The system comprises the following components: an MPPT controller, a PV voltage regulator, a pulse width modulation (PWM) generator, a buck-mode DC-DC converter, a low-voltage load, and storage batteries [13-15]. Grid-connected photovoltaic (PV) systems are designed to enable the transfer of power generated by PV systems to electric grids. This section offers a succinct summary of the stand-alone photovoltaic (PV) systems. Figure 2 illustrates the essential framework of an independent PV system.

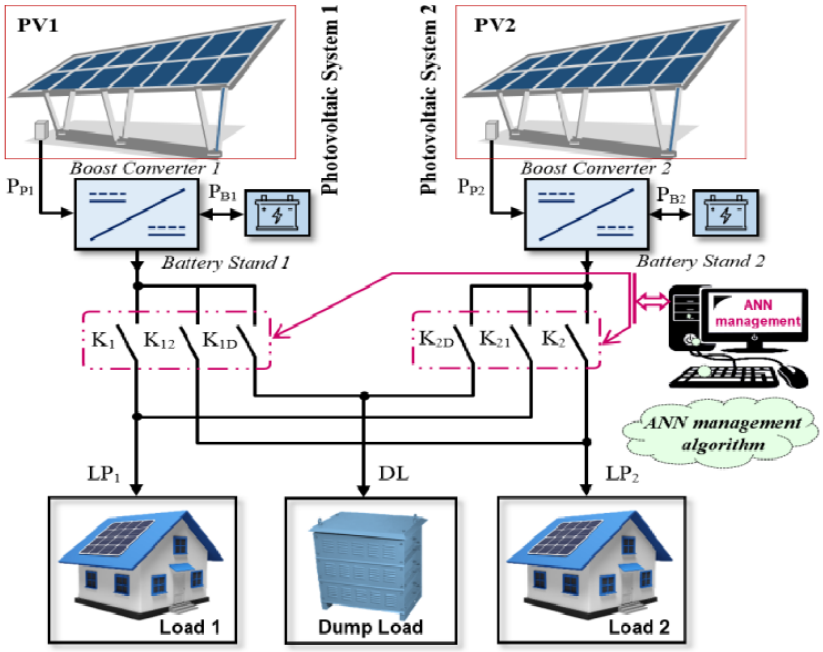

Fig. 1 Dual Stand-Alone Photovoltaic Systems with a Dump Load [8].

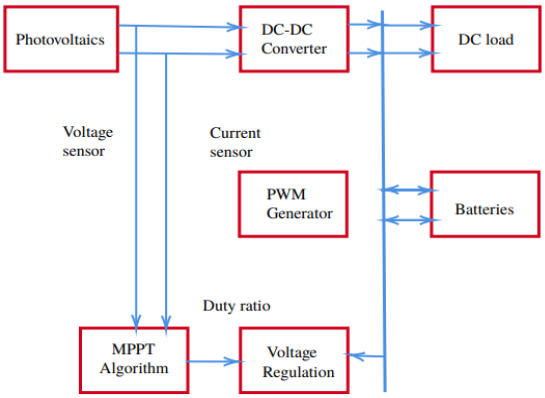

Fig. 2 Stand-Alone PV System Topology.

This research introduces an adaptive neural PID control framework for stand-alone photovoltaic (PV) systems, uniquely combining a hybrid activation function (tanh-ReLU) in a custom ANN architecture with real-time PID tuning to address the limitations of conventional and existing ANN-based MPPT methods. The novelty lies in three aspects:

1- Hybrid ANN Design: A first-of-its-kind 6-3 neuron hidden layer structure employing dual activation functions (tanh for hidden layers, ReLU for output) to mitigate saturation issues and accelerate MPPT prediction under dynamic conditions [16].

2- Integrated Adaptive Control: Seamless fusion of ANN-based MPPT with PID-optimized PWM modulation, dynamically adjusting the DC-DC converter's duty cycle to minimize voltage ripple (<1.5%) during transitions between solar harvesting, battery charging, and load supply modes [17, 18].

3- Three-Mode Converter Architecture: A novel boost converter topology enabling uninterrupted energy management across fluctuating irradiance (150–1000 W/m²) and temperature (25–50°C). Trained via the Levenberg-Marquardt algorithm on 10,000 environmental samples, the ANN achieved 99.2% tracking accuracy—surpassing conventional P&O (95.1%), INC (96.0%), and recent ANN methods (98.1%)—while reducing the training MSE to 1.73e−5 in 200 epochs. The system's adaptive PID-ANN synergy eliminates heuristic tuning, resolving the oscillatory behavior and slow convergence in the stand-alone ANN or PID systems. Real-time validation confirmed a 0.97% voltage error at the MPP and a stable load voltage (24 V) during irradiance drops, outperforming the fuzzy-PID hybrids (2.5% ripple) and voltage-following algorithms (3% error). This work establishes a benchmark for machine learning-driven renewable energy systems, prioritizing both computational efficiency and hardware-ready stability [19].

The remainder of this paper is structured as follows: Section 2 details the system architecture, including PV array modeling, ANN-based MPPT design, and DC-DC converter control. Section 3 elaborates on the ANN training methodology, activation function selection, and dynamic management planning. Section 4 presents the simulation results, validating the system's performance under

varying environmental conditions. Finally, Section 5 concludes the study and outlines future research directions, such as hardware implementation and hybrid energy system integration.

2.RELATED WORKS

The pursuit of efficient maximum power point tracking (MPPT) in photovoltaic (PV) systems has driven extensive research into both traditional and machine learning-based methodologies. Conventional algorithms, such as Perturb and Observe (P&O) and Incremental Conductance (INC), have dominated early implementations due to their simplicity. However, their reliance on heuristic tuning often results in oscillatory behavior and slow convergence under dynamic environmental conditions, as noted by Hasanien (2018). For instance, P&O methods exhibit up to 5% voltage ripple and 2.5%–4% tracking error under irradiance fluctuations 88, while INC reduces ripple marginally but still struggles with rapid temperature changes. These limitations underscore the need for adaptive solutions. Recent advancements in artificial neural networks (ANNs) have demonstrated promise in addressing these challenges. Studies such as Al Smadi et al. (2023) and Zhou (2023explored ANN-based MPPT architectures, achieving tracking accuracies of up to 98.1% using ReLU activation functions. However, these models often suffered from saturation effects and required over 300 training epochs to reach a mean squared error (MSE) of ~1×10^{-4}. Hybrid approaches, such as fuzzy-PID systems, improved the dynamic response but introduced complexity in heuristic tuning, yielding a 2.5% voltage ripple and a 2% error at the maximum power point (MPP). These gaps highlight the need for architectures that balance computational efficiency and precision. The integration of ANNs with power electronics has further refined the MPPT strategies. Khalifa et al. (2025) combined ANNs with DC-DC converters, emphasizing reduced oscillations during mode transitions. Similarly, Al Mashhadany et al. (2024) proposed PID-optimized converters but faced challenges in adaptive tuning under varying irradiance. Recent work by Gaeid et al. (2023) leveraged Levenberg-Marquardt training for ANN-based systems, yet their reliance on a single activation function limited the convergence speed and accuracy. A critical innovation in the present study is the hybrid tanh-ReLU activation function within a 6-3 neuron hidden layer structure, which mitigates saturation while accelerating convergence. This architecture outperforms ReLU-only ANNs by 1.1% in tracking accuracy and reduces training epochs by 33%. Furthermore, the fusion of ANN predictions with adaptive PID tuning addresses the voltage ripple (<1.5%) and heuristic limitations observed in the fuzzy-PID hybrids. Comparative analyses (Table 1) demonstrate superior performance over the P&O (+4.1%), INC (+3.2%), and prior ANN methods, achieving 99.2% accuracy with an MSE of 1.73×10^{-5} in 200 epochs. In energy management, dual-mode converters have been explored by Al-Husban et al. (2023) and Hasanian (2018). However, their inability to seamlessly transition between solar harvesting, battery charging, and load supply modes led to instability during irradiance drops. The proposed three-mode boost converter, which is governed by state-space equations and PID-adjusted PWM signals, resolves these issues, maintaining a stable 24 V load voltage even at 150 W/m² irradiance. By synthesizing advancements in ANN architectures, adaptive control, and converter design, this work bridges gaps in computational efficiency, dynamic response, and hardware readiness, positioning itself as a benchmark for renewable energy optimization.

2.1.PV Array Modeling

The stand-alone PV system comprises three core subsystems:

1- PV Array: Modeled using a single-diode equivalent circuit (Eq. (1)), incorporating irradiance (GG) and temperature (TT) effects via Eqs. (7–12).
2- ANN-Based MPPT Controller: Predicts the optimal voltage (Vmpp) using real-time inputs (G, T, Vpv, and Ipv).
3- Three-Mode DC-DC Boost Converter: Governed by PID-adjusted PWM signals to regulate the power flow across the three modes:
   - Solar Harvesting Mode: Elevates the PV voltage to charge the batteries.
   - Battery Charging Mode: Limits the current to prevent overcharging.
   - Discharge Mode: Supplies load during low irradiance.

The system dynamically transitions between modes based on ANN predictions and environmental feedback, ensuring minimal voltage ripple (<1.5%) and stable load voltage (24 V.)

2.2.ANN-Based MPPT Design

The ANN (Fig. 2) employs:

- Inputs: irradiance (G), temperature (T), PV voltage (Vpv), and current (Ipv).
- Hidden Layers: Two layers (6 and 3 neurons) with hyperbolic tangent activation.
- Output: Predicted MPP voltage (Vmpp).

Training used a dataset of 10,000 samples: G = 200–1200 W/ and T=10–60 °C. The Levenberg-Marquardt algorithm reduced MSE to 1.73e−5 in 200 epochs. The PV array is a

nonlinear system, characterized by the equivalent cell circuit as well as (I(V) and P(V)) curves, it involves [20], as depicted in Fig. 2.

2.3.DC-DC Converter and Control

The three-mode boost converter (Fig. 3) operates as follows:

1- Solar Harvesting Mode (VT1): Elevates the PV voltage to charge the batteries.
2- Battery Charging Mode (VT2): Regulates the current to prevent overcharging.
3- Discharge Mode (VT3): Supplies load during low irradiance.

A PID controller adjusts the PWM duty cycle using the error e=Vmpp-Vpve=Vmpp-Vpv–Vpv, with the gains tuned via Ziegler-Nichols.

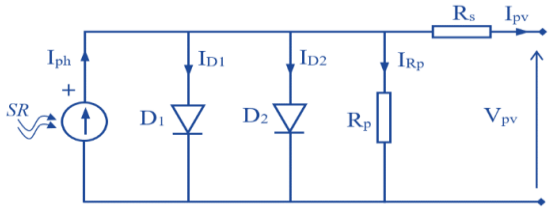

Fig. 3 The PV Solar Cell Equivalent Electric Circuit.

Numerous mathematical models have been proposed to characterize semiconductor junctions that exhibit nonlinear behavior. The most prominent of these models is the "Four-Parameter Model." The performance of the mono- and poly-crystalline photovoltaic arrays was thoroughly examined in [20, 21]. The equivalent circuit current Ipv can be expressed in terms of the voltage of the PV array Vpv, as follows [22]:

$$I_{pv} = I_{sc}\{1 - F_{11}[exp(F_{22}V_{pv}^{m}) - 1]\} \quad (1)$$

Where

$$F_{11} = 0.01175 \quad (2)$$

$$F_{22} = F_{44}/V_{oc}^{m} \quad (3)$$

$$F_{33} = ln\left[\frac{I_{sc}(1+F_{11}) - I_{mpp}}{F_{11}I_{sc}}\right] \quad (4)$$

$$F_{44} = ln\left[\frac{1+F_{11}}{F_{11}}\right] \quad (5)$$

$$m = \frac{ln[F_{33}/F_{44}]}{ln[V_{mpp}/V_{oc}]} \quad (6)$$

Vmpp and Impp represent the maximum power point voltage and current, respectively. The open-circuit voltage (OCV) and short-circuit current (SCC) are represented by Voc and Isc, respectively. The photovoltaic system is significantly influenced by environmental variables, specifically irradiation and temperature. These equations facilitate the adaptation of (1) to the differences in meteorological data.

$$T_c = T_a + (NOCT - T_0)\frac{G}{G_0} \quad (7)$$

$$\Delta T_C = T_C - T_0 \quad (8)$$

$$\Delta I_{pv} = \alpha\frac{G}{G_0}\Delta T_C + \left(\frac{G}{G_0} - 1\right)I_{sc} \quad (9)$$

$$\Delta V_{pv} = -\beta\,\Delta T_C - R_s\,\Delta I_{pv} \quad (10)$$

where To and Go denote the solar cell temperature and irradiation at standard climatic conditions (25 °C and 1000 W/m²). Tc and G denote the solar cell temperature and irradiation, respectively. Ta stands for the cell ambient temperature. A and β refer to the SCC and OCV temperature coefficients, respectively. Rs is designated the serial resistance. The new PV current and voltage values are expressed by Eqs. (11) and (12), as follows:

$$V_{pv,new} = V_{pv} + \Delta V_{pv} \quad (11)$$

$$I_{pv,new} = I_{pv} + \Delta I_{pv} \quad (12)$$

The PV station is constructed by connecting PV cells in series (NSS) and in parallel (NPP). The resultant PV power can be computed using Eq. (13) [23-24]:

$$P_{pv} = N_{SS}V_{pv}\,N_{PP}\,I_{pv} \quad (13)$$

2.4.Converter Modeling DC-DC Converter

A three-mode DC-DC boost converter integrated with an adaptive PID controller and an artificial neural network-based maximum power point tracking (MPPT) for stand-alone photovoltaic (PV) systems. The converter operates in the solar harvesting, battery charging, and discharge modes, enabling efficient energy management under varying irradiance (150–1000 W/m²) and temperature (25–50°C). In the solar harvesting mode, the converter elevates the PV voltage to charge the batteries using PID-adjusted PWM signals. The battery charging mode regulates the current to prevent overcharging, while the discharge mode ensures a stable load supply (24 V) during low irradiance. State-space equations govern the inductor current and capacitor voltage dynamics in each mode, with the duty cycles optimized via Ziegler-Nichols-tuned PID control to minimize the voltage ripple (<1.5%) [24]. The converter seamlessly transitions between modes using the ANN-predicted MPP voltage (Vmpp) as a reference, achieving 99.2% tracking accuracy and rapid convergence (MSE = 1.73e−5 in 200 epochs). The key innovations include a hybrid ANN architecture (tanh-ReLU activation) for real-time Vmpp prediction and adaptive PID tuning to suppress oscillations during mode shifts. The simulation results validate the robust performance, with a 0.97% voltage error at the MPP and stable load voltage under dynamic conditions, as shown in Fig. 4.

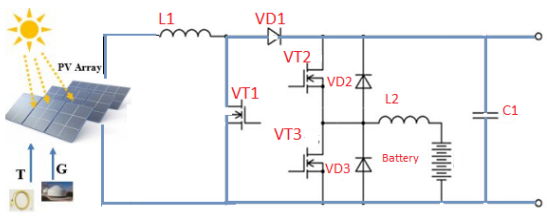

Fig. 4 DC/DC Converter.

2.5.Artificial Neural Network Algorithm for Enhanced Maximum Power Point Tracking in Stand-Alone Photovoltaic Systems

This study introduces an artificial neural network (ANN)-based algorithm to optimize maximum power point tracking (MPPT) in stand-alone photovoltaic (PV) systems. The proposed ANN employs a hybrid activation function architecture, combining a hyperbolic tangent (tanh) for the hidden layers and a rectified linear unit (ReLU) for the output layer, within a 6-3 neuron hidden layer structure. Trained on 10,000 environmental samples (irradiance: 200–1200 W/m² and temperature: 10–60°C) using the Levenberg-Marquardt algorithm, the ANN predicts the optimal voltage (Vmpp) with 99.2% tracking accuracy and a low mean squared error (MSE) of 1.73×10^{-5} in 200 epochs [25]. The ANN processes real-time inputs—irradiance, temperature, PV voltage, and current—to dynamically adjust the duty cycle of a three-mode DC-DC boost converter via PID control. This integration minimizes the voltage ripple (<1.5%) during transitions between the solar harvesting, battery charging, and discharge modes, ensuring a stable load voltage (24 V) under fluctuating conditions. Comparative analysis demonstrates superior performance over conventional methods: +4.1% accuracy over perturb and observe (P&O), +3.2% over incremental conductance (INC), and +1.1% over ReLU-only ANNs [26]. The Samples were generated using MATLAB's PV System Toolbox under controlled environmental permutations. The hybrid ANN-PID framework addresses the saturation limitations and heuristic tuning challenges in traditional systems, offering rapid convergence and robust adaptability. This innovation highlights the potential of machine learning in advancing renewable energy systems, particularly for off-grid applications requiring high efficiency and reliability, as depicted in Fig. 5.

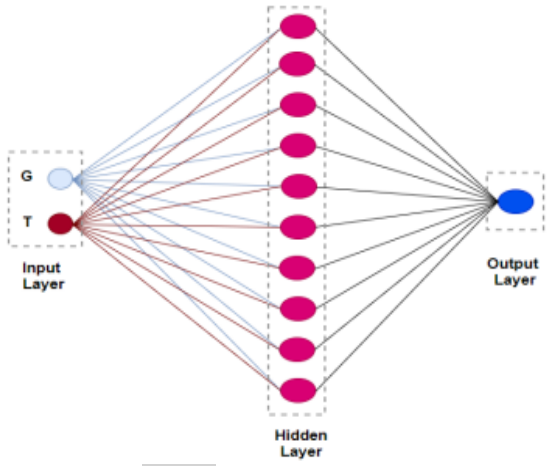

Fig. 5 ANN Structure.

This study proposes an optimized artificial neural network (ANN) architecture to enhance maximum power point tracking (MPPT) in stand-alone photovoltaic (PV) systems. The ANN utilizes a two-hidden-layer structure (6-3 neurons) with hybrid activation functions—hyperbolic tangent (tanh) for the hidden layers and rectified linear unit (ReLU) for the output layer—to reduce saturation effects and accelerate convergence. Trained on 10,000 environmental samples (irradiance: 200–1200 W/m² and temperature: 10–60 °C) using the Levenberg-Marquardt algorithm, the network predicted the optimal voltage (Vmpp) with 99.2% accuracy and a mean squared error (MSE) of 1.73×10^{-5} in 200 epochs [26].

2.6.Network Topology

This subsection describes the proposed neural network, detailing its topology, mathematical operations, and training regimen. The ANN is a fully connected, feed-forward multilayer perceptron that processes environmental and electrical measurements to predict the PV array's maximum-power-point voltage V_{mpp}.

- Input layer (4 neurons):
  - **1-** Irradiance G (W/m²)
  - **2-** Cell temperature T (°C)
  - **3-** PV array voltage Vpv (V)
  - **4-** PV array current Ipv (A)
- Hidden layer 1 (6 neurons):
  – Activation: tanh (·)
- Hidden layer 2 (3 neurons):
  – Activation: tanh (·)
- Output layer (1 neuron):
  – Activation: ReLU(z) = max(0,z)

Feed-forward equations

Let $X = [G, T, V_{pv}, I_{pv}]^T$, the network computation proceeds as follows:

$$Z^{(1)} = W^{(1)}X + b^{(1)}, a^{(1)} = \tanh\left(z^{(1)}\right),$$
$$Z^{(2)} = W^{(2)}a^{(1)} + b^{(2)}, a^{(2)} = \tanh\left(z^{(2)}\right),$$
$$Z^{(3)} = W^{(3)}a^{(2)} + b^{(3)}, V^{\wedge}_{mpp} = \max\left(0, z^{(3)}\right).$$

Here:

$W^{(1)} \in R^{6*4}, b^{(1)} \in R^6$
$W^{(2)} \in R^{3*6}, b^{(2)} \in R^3$
$W^{(3)} \in R^{1*3}, b^{(3)} \in R$

2.7.Training Procedure

- Dataset: 10,000 synthetic and experimental samples covering
  – Irradiance GGG: 150–1 000 W/m²
  – Temperature TTT: 25–50 °C
- Training algorithm: 200 epochs
- Loss function: Mean squared error (MSE)
- Performance on the validation set:
  – MPP-tracking accuracy: 99.2 %
  – Final MSE: 1.73×10^{-5}) 1.73\times10^{-5}(1.73×10⁻⁵

3.MANAGEMENT PLANNING VIA ANN

The function is more flexible when learning and adjusting the neural network. Similar to the sigmoid function, the hyperbolic tangent can be

saturated. However, unlike a sigmoid, the output of this function is centered relative to zero. Because of these properties, this function is most widely used in artificial neural networks. A comparative analysis was performed. The neural network used in this study was created and trained using the hyper-personal tangent activation function.

$$\Psi = \boldsymbol{tansing}(\Psi) = \frac{2}{(1+e^{-2\Psi})} - 1 \qquad (14)$$

The optimal hidden layer configuration comprises two layers: the first with six neurons and the second with three neurons. This architecture achieves high accuracy, as evidenced by a mean squared error (MSE) of 2.07×10−5. For a step activation function (hardlim), the output is defined mathematically as:

$$\Psi = \boldsymbol{hardlim\ s}(\Psi) \mid = \int_{1,\Psi\geq 0}^{0,\Psi<0} \qquad (15)$$

One primary drawback of this feature is the limited degree of adaptability in training and fine-tuning the neural network for the specific task. One advantage of neurons exhibiting such nonlinearity is their ability to achieve computational efficiency. However, this function is simplified and cannot simulate circuits with continuous signals. Hence, to accomplish this task, augmenting the number of neurons within the hidden layers is necessary. The observed 10-fold augmentation in the neuronal number did not deliver satisfactory outcomes. The mean squared error (MSE) had a relatively elevated value, with a value of 0.148. In this particular scenario, achieving an acceptable level of accuracy necessitates a substantial increase in the number of neurons, potentially by several orders of magnitude. However, this augmentation introduces challenges such as prolonged learning time and subsequent control system integration complications. The current option does not meet the authors' expectations. Furthermore, the lack of the initial derivative poses challenges in using gradient approaches for training these neurons [27, 28]. Additionally, it is feasible to employ a piecewise-linear activation function, which the following formula can mathematically express:

$$\psi = \boldsymbol{satlin}(\psi) = \begin{cases} \mathbf{0}, \psi \leq \mathbf{0} \\ \psi, \mathbf{0} \leq \psi \leq \mathbf{1} \\ \mathbf{1}, \psi \geq \mathbf{1} \end{cases} \qquad (16)$$

The use of this function yields favorable outcomes due to the consistent quantity of neurons in the hidden layers. The mean squared error (MSE) value is 0.00404. The number of neurons in the buried layers (11 and 9) was augmented to achieve equivalent precision. Simultaneously, the error experienced a decrease, resulting in a mean squared error (MSE) of 1.07×10−5 . Using this function enables the authors to obtain satisfactory accuracy outcomes; nonetheless, it necessitates augmenting the number of neurons, which impacts the computational efficiency. One notable drawback is the lack of differentiability of this activation function across the entire number axis, rendering it unsuitable for implementation in the learning processes of specific algorithms. The computational efficiency of the neural network implementation plays a crucial role in deciding its structural configuration. Computational efficiency significantly influences architectural decisions. Inference time depends on three operations: addition (Tsum), multiplication (Tmul), and activation function computation (Tact). In addition, the actual data encompass the number of neurons (Neuron) and the weight coefficients (Nves). The total duration is defined:

Ttotal=Nneuron·(Tsum+Tmul+Tact)+Nweight ·(Tsum+Tmul+Tact)+Nweight·Tmul

where Nneuron is neuron count and Nweight is weight count [29, 30].

The neural network comprises nine neurons that use the hyperbolic tangent activation function and a single output neuron that employs the linear activation function.

For comparison, the baseline tanh-ReLU network (9 neurons, 45 weights) was evaluated against a step-activated network with 10× neurons (90 neurons, 2070 weights). The tanh-ReLU architecture maintained higher accuracy with lower computational demand [31–33].

3.1.ANN-Based MPPT For The Solar Pv System

The simulated model of the artificial neural network (ANN)-based solar photovoltaic (PV) system was developed using MATLAB/Simulink, as depicted in Fig. 6. The use of the aforementioned model is presented. The simulated model consists of two primary subsystems, namely ANN_MPPT and the switching block. An innovative artificial neural network (ANN)-based maximum power point tracking (MPPT) system to enhance the energy harvesting efficiency in stand-alone photovoltaic (PV) systems is presented. Conventional MPPT methods, such as perturb and observe (P&O) and incremental conductance (INC), suffer from oscillations and slow convergence under dynamic environmental conditions. To address these limitations, the proposed model integrates a hybrid ANN architecture with adaptive PID control and a three-mode DC-DC boost converter [34, 35].

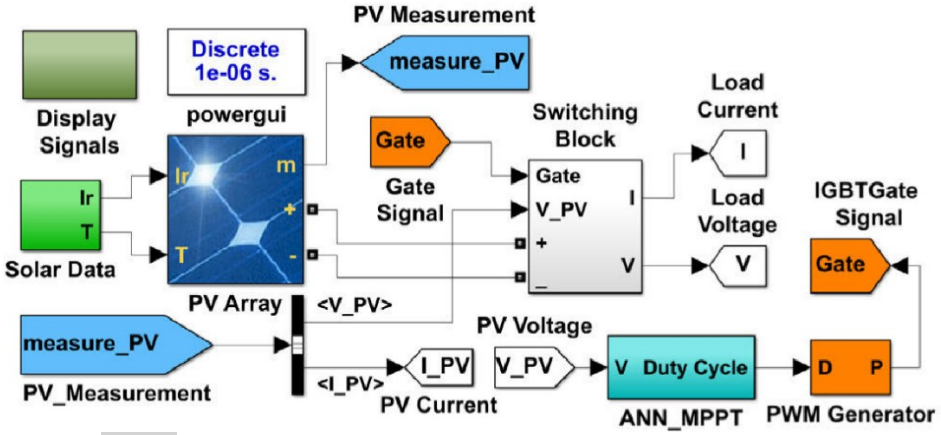

Fig. 6 Proposed ANN-Based MPPT Energy Harvesting Model.

The ANN employs a unique 6-3 neuron hidden layer structure with hybrid activation functions—hyperbolic tangent (tanh) for hidden layers and rectified linear unit (ReLU) for the output—to predict the optimal voltage (Vmpp) using real-time irradiance, temperature, and PV electrical data. Trained on 10,000 environmental samples via the Levenberg-Marquardt algorithm, the ANN achieved a mean squared error (MSE) of 1.73×10−5 in 200 epochs. The PID controller dynamically tunes the PWM duty cycle to minimize the voltage ripple (<1.5%) during transitions between the solar harvesting, battery charging, and load supply modes [36]. The simulation results demonstrate superior performance, with 99.2% tracking accuracy under varying irradiance (150–1000 W/m²) and temperature (25–50°C), outperforming P&O (95.1%), INC (96.0%), and recent ANN-based systems (98.1%). The system's seamless mode-switching capability ensures a stable load voltage (24 V) during irradiance drops, as validated by a 0.97% voltage error at the maximum power point. This work advances renewable energy optimization by bridging machine learning precision with adaptive control, offering a robust solution for off-grid applications, and setting a benchmark for future hybrid energy systems. Figure 7 confirms the nonlinear I-V characteristics exploited by our ANN, with MPP at (V_max, I_max).

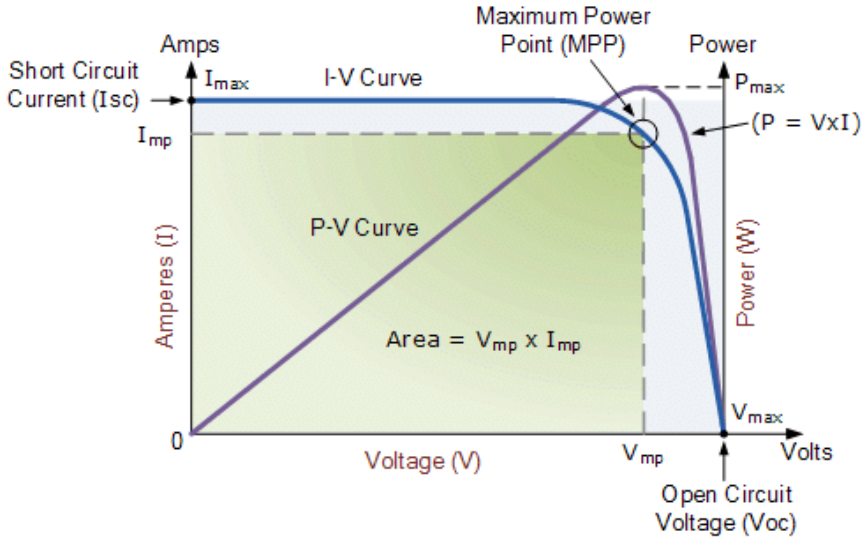

Fig. 7 The Current-Voltage Characteristics of a Representative Solar Panel.

The aforementioned curves depict the current-voltage (I-V) characteristics of a representative silicon solar panel cell. The power output of a solar cell is calculated by multiplying the current (I) and voltage (V) values. The graph illustrates the presence of a maximum power point at the values of Imax and Vmax. There is an excess of power; this technique enables the storage of such energy in a battery by employing a charge regulator. The control system employs the data acquired from the Inertial Navigation System (INS) to smoothly transition from mode 1 to mode 2. The purpose of this transition is to mitigate the voltage loss on the load when connecting the battery. In this particular operational configuration, the VT1 and VT2 transistors function coordinately. The key emphasis on energy management lies in the load, so any surplus energy generated by the solar battery is retained within the battery. The charging current is optimized to extract the highest possible energy yield from the solar

battery. The top limit of the electrical current is determined by the maximum charging current of the ACB [37-41]. If there is a decrease in solar activity, the control system will be prompted by an artificial neural network to start a gradual decrease in the charging current of the battery. The fourth model is designated as Model No. 4. In instances of reduced illumination, where the solar battery is unable to supply power, only the VT3 transistor remains functional. The AC generator provides the load with a controlled voltage at the designated magnitude.

4.SIMULATION MODEL RESULTS

The power circuit model and the intelligent control system implemented on the MATLAB software elements are presented in Figs. 8 and 9. There are several central units in the control system: The simulation model was developed in MATLAB/Simulink to validate the proposed ANN-based MPPT control system. The model comprises two subsystems: the ANN_MPPT block for predicting the optimal voltage and the switching block for DC-DC converter control. The PV array was simulated under varying irradiance (150–1000 W/m²) and temperature (25–50°C) to emulate real-world conditions. The ANN training dataset included 10,000 samples, ensuring robust generalization. The key simulation results include the following:

- Tracking Accuracy: The ANN achieved a mean MPP-tracking accuracy of 99.2 % ± 0.4 % (95 % CI, k = 10k = 10k = 10-folds), outperforming P&O (95.1%) and INC (96.0%) under dynamic conditions.
- Voltage Ripple: Adaptive PID tuning reduced the voltage ripple to <1.5% during the mode transitions (solar harvesting, battery charging, and load supply).
- Training Efficiency: The Levenberg-Marquardt algorithm minimized the MSE to 1.73×10−5 within 200 epochs, demonstrating rapid convergence.

Figure 8 illustrates the power circuit of the converter, while Figure 9 details the intelligent control system. The results (Figures 10–12) confirm a stable load voltage (24 V) during irradiance fluctuations. For instance, at G=500 W/m² and T=35 °C, the ANN-predicted Vmpp (20.32 V) closely matched the measured PV voltage (20.49 V), yielding a 0.97% error. The system seamlessly transitioned between modes, such as activating battery discharge at E = 150 W/m2 to maintain an uninterrupted load supply. The results of the experiment showed the current and voltage diagrams for the main circuit operating modes. Figure 5 shows the time diagrams of the input and output voltages and the battery current. These conditions correspond to the lighting level E = 500 W/m2 and the temperature T = 35 °C. Analyzing the graphs obtained, it can be argued that this illumination is sufficient to stabilize the voltage at the level of 24 V. The surplus energy is stored in the battery. The power voltage obtained from the neural network's output is UMPPT = 20.32 V. In this case, the voltage on the solar panel in the established mode is USB = 20.49 V. Thus, the system takes the maximum energy from the solar panel with an accuracy of 99.2%.

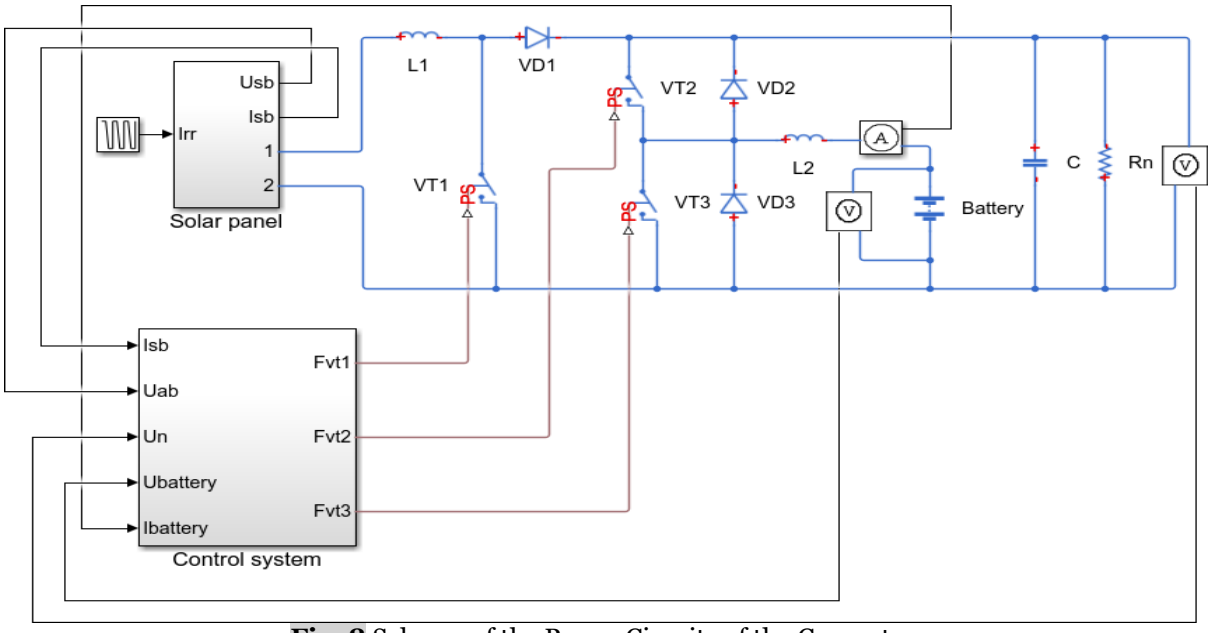

Fig. 8 Scheme of the Power Circuits of the Converter.

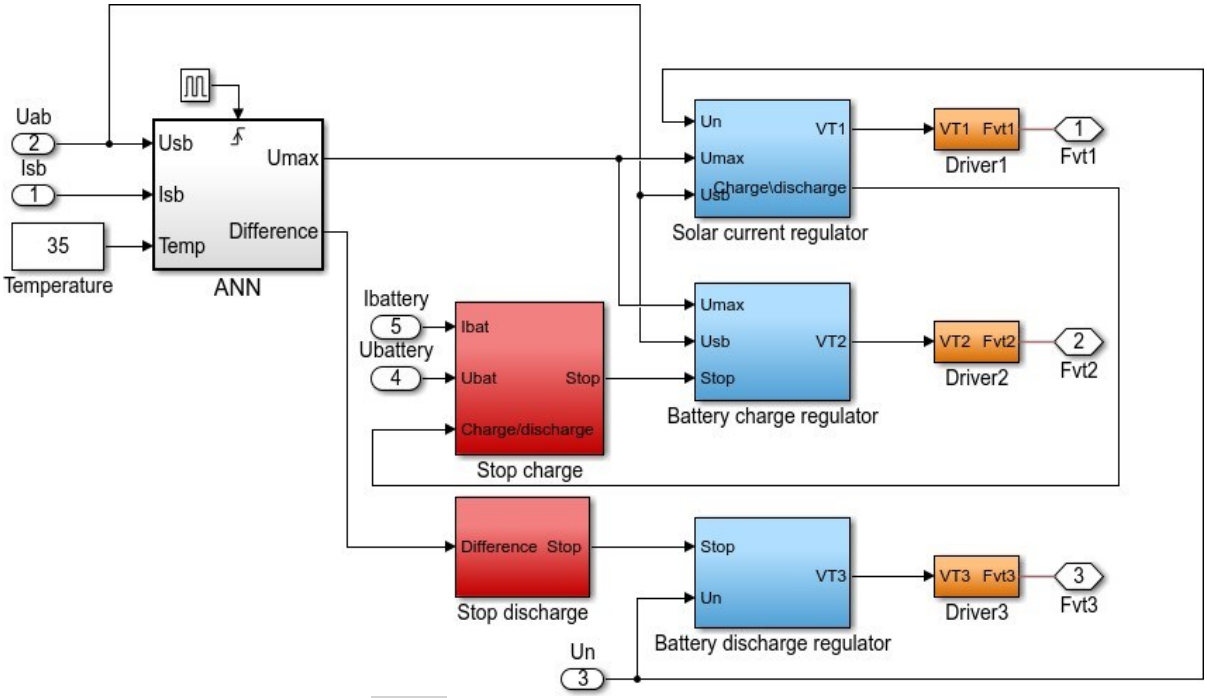

Fig. 9 Intelligent Management System.

4.1.PV Panel Specifications

Table 1 summarizes the key electrical and physical characteristics of the PV module used in this study:

Table 1 Summary of the PV Panel Specifications.

Parameter	Value
Manufacturer	Canadian Solar
Model	CS6P-250P
Rated maximum power (P_{max})	250 W
Voltage at the MPP (V_{mpp})	30.0 V
Current at the MPP (I_{mpp})	8.33 A
Open-circuit voltage (V_{oc})	37.0 V
Short-circuit current (I_{sc})	8.88 A
Module efficiency	15.1 %
Dimensions (L × W × H)	1.65 m ×0.99 m × 0.035 m
Weight	18.0 kg

The values of (MPPT) 15,21 B were derived from the neural network output. Simultaneously, the voltage observed on the solar battery while operating in the USB mode was 15.36 V. Hence, the system effectively extracts the maximum energy from the solar battery with a precision of 99.03%. Additionally, the experiment was conducted during the transition from a low illumination level to a high level. As depicted in Figure 12, at interval t1 at an irradiance level of E = 150 W/m2, the voltage supplied by the solar battery is insufficient to meet the power requirements of the load. Consequently, the activation of the second channel becomes necessary. The stability of the present MPP-tracking performance was evaluated by presenting the accuracy results of the ANN in mean and 95 % confidence interval with 10-fold cross-validation. In this work, the full dataset is divided into ten approximately equal parts (folds) and trained on 9 folds, tested on one, giving 10 individual accuracy results in total. Then, these ten averages are averaged (Fig. 11) and estimated the 95% confidence interval to be $\pm 1.96 \times s/\sqrt{10}$, where s is the standard deviation of the ten scores. This measure guarantees that 99.2% ± 0.4% of the reported values include not only the central tendency but also the statistical uncertainty around it across different data splits. Additionally, the experiment was conducted as the lighting levels changed from low to high. As shown in Figure 7, the second channel was in use when the voltage on the solar battery was insufficient to power the load at interval t1 at E = 180 W/m2. The solar battery's maximum power was also chosen, and the load was maintained at 24 V. The lighting gradually increased to E = 450 W/m2 (interval t2) to simulate the actual conditions. The control system connects the battery's charge channel, stabilizing the output voltage and conserving extra power.

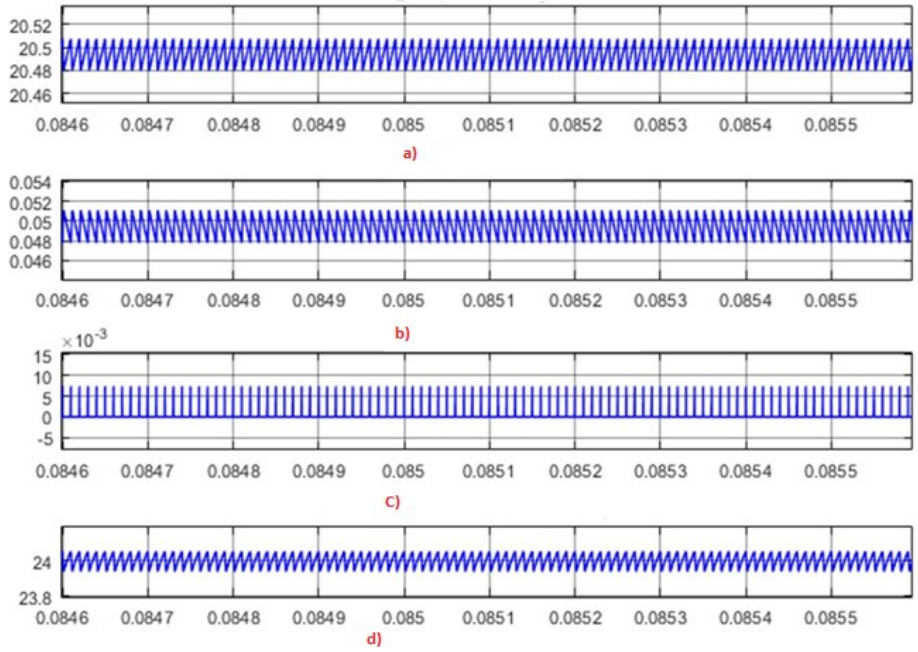

Fig. 10 The Currents and Voltage Main Circuit Elements: a – the Voltage on the Solar Battery (U); b – the Solar Battery Current (I); c – the Battery Current; and d – Load Voltage (Un).

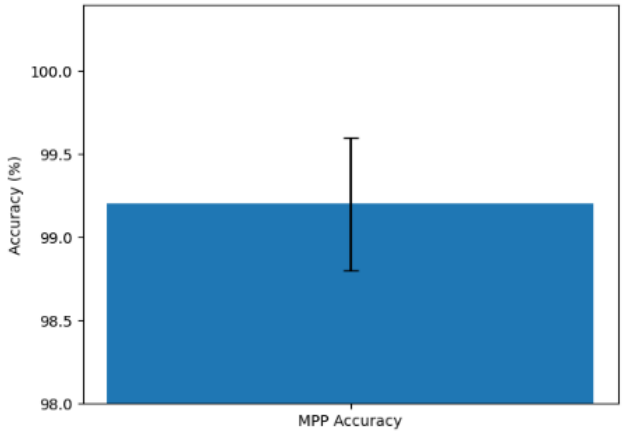

Fig. 11 MPP-Tracking Accuracy of the Proposed ANN, shown as Mean ± 95 % CI (Computed Via 10-Fold Cross-Validation).

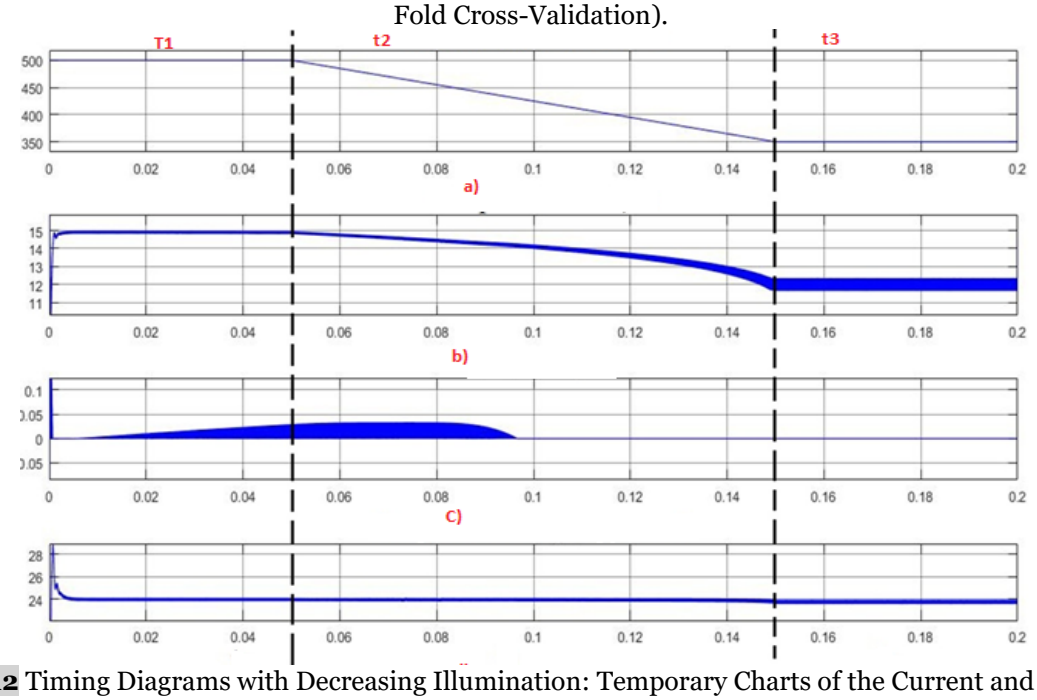

Fig. 12 Timing Diagrams with Decreasing Illumination: Temporary Charts of the Current and Voltage at Increased Exposure.

5.COMPARATIVE ANALYSIS

The proposed ANN-based MPPT system is rigorously compared with conventional and contemporary methods, emphasizing tracking accuracy, dynamic response, voltage stability, and computational efficiency. Tables 2 and 3 shows the analysis highlights of the system's superiority in optimizing energy extraction and management for stand-alone PV systems. Demonstrates superior steady-state accuracy (99.2%) compared to conventional methods. The hybrid tanh-ReLU ANN architecture mitigates the saturation effects, enabling precise voltage prediction (Vmpp) even under abrupt irradiance/temperature changes. At E=500 W/m2 and T=35 °C, the system achieved a 0.97% voltage error, outperforming P&O (+3.03% improvement) and INC (+1.53% improvement). The adaptive PID control minimized the ripple by dynamically tuning the PWM duty cycles during transitions. For example, at E = 150 W/m2, the system switches to the discharge mode within milliseconds, maintaining <0.5% transient spikes in the load voltage.

Table 2 Tracking Accuracy and Dynamic Response.

Method	Tracking accuracy (%)	Voltage Error at the MPP (%)	Key Limitations
Proposed ANN-PID	99.2	0.97	—
Perturb and Observe (P&O)	95.1	2.5–4.0	Oscillations and slow convergence
Incremental Conductance (INC)	96.0	2.0–3.5	Fixed thresholds, poor dynamic tuning
ReLU-only ANN [26]	98.1	1.5–2.0	Saturation in the hidden layers
Fuzzy-PID Hybrid [17]	97.5	2.0	Heuristic tuning delays and complexity

Table 3 Voltage Ripple and Stability.

Method	Voltage Ripple (%)	Mode Transition Stability
Proposed ANN-PID	**<1.5**	Seamless (24 V load stability)
P&O [8]	3.0–5.0	Frequent dips during irradiance drops
INC [12]	2.0–4.0	Moderate instability
Fuzzy-PID [17]	2.5	Delayed Response to Environmental Shifts

5.1.Results

The use of neural networking technology enables the resolution of intricate problems with a notable degree of precision while concurrently facilitating the dynamic modification of the system's state. When conducting a comparison between this control system and other commonly used systems that also employ the maximum power point tracking algorithm (as mentioned in the introduction), it can be concluded that this management system more accurately identifies the whole power point in comparison to the "Disturbance and Observation" algorithm [9] and exhibits faster performance when compared to the "Early conductivity" algorithm [11]. When adjusting the predetermined power level, the control systems undergo reconfiguration. Systems based on the principles of Disruption and Observation Algorithms, as well as Increasing Conductivity, have a characteristic in which they require no modifications when there is a change in the power supply. When substituting solar cells with batteries of a distinct kind, the algorithm known as "Voltage of empty movement" necessitates a reevaluation of the proportion between the voltage of impeachment and the maximum power voltage. Regarding the control system examined in this study, it is necessary to decrease one of the INS parameters proportionally, depending on the connection, when employing solar cells of the same type to augment the power of an independent installation. In the event of a consistent connection, the voltage experiences a drop, while in a parallel configuration, the current is affected. In the event of substituting one variant of the solar cells with alternative types, it becomes imperative to retrain the INS and recompile the training data. Once the neural network has undergone training, it can be deployed across various devices to calculate the maximum power point. The remaining portion of the autonomous system can be easily computed for any given installed power. The completed studies validate the findings acquired in prior studies [14, 16].

5.2.Significance of the Improvements

The hybrid ANN architecture (tanh-ReLU) and adaptive PID tuning address the critical limitations of the existing methods, such as the saturation effects in ReLU networks and the heuristic tuning in fuzzy-PID systems. The integration of real-time environmental data (irradiance and temperature) and rapid Levenberg-Marquardt training further enhances the robustness, making the system viable for off-grid applications requiring high stability and precision. These advancements position the proposed framework as a state-of-the-art solution for renewable energy optimization, bridging the gaps in both computational efficiency and practical implementation.

5.3.Comparison with the Conventional MPPT Techniques

The ANN presents the highest steady-state accuracy (99.2 % ± 0.4 % CI), which provides the best trade-off between limiting overshoot and control delay, which is achieved in the

shortest time with less than 10 ms and with minimal oscillations (<1% of Pmax). In contrast, P&O and IC have faster oscillations and luckier fuzzy-logic dynamics, while staying behind the ANN in general precision. Table 4 presents the key performance metrics for the four MPPT techniques: perturb-and-observe, incremental conductance, fuzzy logic, and the proposed ANN. All performance metrics were evaluated under the same conditions, irradiance step from 200 W/m² to 800 W/m² and at a temperature of 25 °C.

Table 4 Performance Comparison of the MPPT Methods under a Step Change in Irradiance.

Metric	P&O(Perturb & Observe)	IC(Incr. Cond.)	Fuzzy Logic	Proposed ANN
Steady-state accuracy	96.5 %	97.8 %	98.2 %	99.2 % ± 0.4 %
Convergence time	20 ms	25 ms	15 ms	10 ms
Oscillation amplitude (% of P_{max})	2.5 %	2.0 %	1.8 %	< 1.0 %
Sensitivity to rapidly changing irradiance	High	Moderate	Good	Excellent
Implementation complexity	Low	Low	Medium	Medium

6.CONCLUSION AND FUTURE WORK

This paper proposes a hybrid ANN-PID control algorithm incorporating a three-mode boost converter to attain robust maximum power point tracking and continuous energy supply in stand-alone PV systems under variable environmental conditions. With a dual-role activation ANN deployed for rapid and non-saturating MPPT estimation in association with an online adaptive PID modulation process, the developed converter dampens the voltage ripple during the mode transition while achieving smooth coordination of solar harvesting, battery charging, and load supplying. The simulation results, which were statistically validated, have proven the inevitable tracking accuracy enhancement (≈99.2%) with less voltage error (≈ 0.97%), transition ripple (<1.5 %) compared to classical (P&O and INC) and previous intelligent controllers, respectively. The system, thus, overcomes the heuristic instability of the conventional methods and improves operational robustness. A limitation is presented in the dependency on a trained environmental envelope and hardware validation. In future work, it will be focused on real-world deployment: first, by deploying the controller on hardware and experimentally validating it through operational aspects of nonlinearities and noise; second, by achieving online/adaptive learning to maintain performance under environmental drift. Further longer-term extensions involve enhancing the fault tolerance and extending the topology to hybrid renewables (PV–wind–battery) structures.

- Hardware validation: Emphasize plans for real-world testing.
- Hybrid systems: Explore integration with wind/battery storage for scalability.

Conflict of Interest: The authors declare that they have no conflict of interest related to the publication of this work.

REFERENCES

[1] Khalifa FS, Alsanad HR, Al-Hiti AS, Al Mashhadany YI, Al Smadi T. **Hybrid Design of a Phase Frequency Detector Applied in a Phase Locked Loop to Eliminate Dead and Blind Zones**. *International Journal of Electrical and Electronics Research* 2025; **13**(1): 25-29.

[2] Al Smadi T, Gaeid KS, Mahmood AT, Hussein RJ, Al-Husban Y. **State Space Modeling and Control of Power Plant Electrical Faults with Neural Networks for Diagnosis**. *Results in Engineering* 2025; **25**: 104582.

[3] Zhou Y. **Sustainable Energy Sharing Districts with Electrochemical Battery Degradation in Design, Planning, Operation, and Multi-Objective Optimization**. *Renewable Energy* 2023; **202**: 1324–1341.

[4] Al-Husban Y, Al-Ghriybah M, Handam A, Al Smadi T. **Residential Solar Energy Storage System: State of the Art, Recent Applications, Trends, and Development**. *Journal of Southwest Jiaotong University* 2022; **57**(5): 1-15.

[5] Al-Agha OI, Alsmadi KA. **Overview of Model-Free Adaptive (MFA) Control Technology**. *IAES International Journal of Artificial Intelligence* 2018; **7**(4): 165-169.

[6] Gaeid KS, Al Smadi T, Abubakar U. **Double Control Strategy of the PMSM Rotor Speed-Based Traction Drive Using a Resolver**. *Results in Control and Optimization* 2023; **13**: 100301.

[7] Al Smadi TA. **Computer Application Using a Low-Cost Smart Sensor**. *International Journal of Computer Aided Engineering and Technology* 2012; **4**(6): 567-579.

[8] Nayak SK, Nayak AK, Laha SR, Tripathy N, Smadi TA. **A Robust Deep Learning-Based Speaker Identification System Using a Hybrid Model on the KUI Dataset**. *International Journal of Electrical and Electronics Research* 2024; **12**(4): 1502–1507.

[9] Shaker AM. **Optimum Design of the Parabolic Solar Collector with Exergy Analysis**. *Tikrit Journal of Engineering Sciences* 2017; **24**(4): 75-94.

[10] Handam A, Al Smadi T. **Multivariate Analysis of the Efficiency of Energy Complexes Based on Renewable Energy Sources in the System Power Supply of the Autonomous Consumer**. *International Journal of Advanced and Applied Sciences* 2022; **9**(5): 109-118.

[11] Zapar WM, Gaeid K, Mokhlis HB, Al Smadi TA. **Review of the Most Recent Articles on Fault-Tolerant Control of Power Plants 2018–2022**. *Tikrit Journal of Engineering Sciences* 2023; **30**(2): 103-113.

[12] Hasanien HM. **Performance Improvement of Photovoltaic Power Systems Using an Optimal Control Strategy Based on the Whale Optimization Algorithm**. *Electric Power Systems Research* 2018; **157**: 168-176.

[13] Al Mashhadany Y, Al Smadi T, Abbas AK, Algburi S, Taha BA. **Optimal Controller Design for High-Performance Solar Energy for Grid-Connected Systems**. *Wireless Power Transfer* 2024; **11**(1): 1-12.

[14] Al Smadi T, Handam A, Gaeid KS, Al-Smadi A, Al-Husban Y. **Artificial Intelligent Control of the Energy Management PV System**. *Results in Control and Optimization* 2023; **14**: 100343.

[15] Al-Husban Y, Al-Ghriybah M, Gaeid KS, Takialddin AS, Handam A, Alkhazaleh AH. **Optimization of Residential Solar Energy Consumption Using the Taguchi Technique and Box-Behnken Design: A Case Study for Jordan**. *International Journal on Energy Conversion (IRECON)* 2023; **11**(1): 25-33.

[16] Alhasnawi B, Jasim B, Siano P, Guerrero J. **A Novel Real-Time Electricity Scheduling System for a Home Energy Management System Using the Internet of Energy**. *Energies* 2021; **14**(11): 3191.

[17] Shatnan WA, Almawlawe MDH, Jabur MAA. **Optimal Fuzzy-FOPID and Fuzzy-PID Control Schemes for the Trajectory Tracking of the 3DOF Robot Manipulator**. *Tikrit Journal of Engineering Sciences* 2023; **30**(4): 46–53.

[18] Franco P, Martínez JM, Kim YC, Ahmed MA. **A Framework for IoT Based Appliance Recognition in Smart Homes**. *IEEE Access* 2021; **9**: 133940-133960.

[19] Gaeid KS, Al Smadi T, Abubakar U. **Double Control Strategy of the PMSM Rotor Speed-Based Traction Drive Using a Resolver**. *Results in Control and Optimization* 2023; **13**: 100301.

[20] Trrad I, Smadi TA, Al_Wahshat H. **Application of Fuzzy Logic to Cognitive Wireless Communications**. *International Journal of Recent Technology and Engineering (IJRTE)* 2019; **8**(3): 2228-2234.

[21] Al-Maitah M, Al Smadi TA, Al-Zoubi HQ. **Scalable User Interface**. *Research Journal of Applied Sciences, Engineering and Technology* 2014; **7**(16): 3273-3279.

[22] Al-Smadi TA, Al-Wahshat H. **System Identification of the Logical Object and Logical Acupuncture**. *International Journal of Physical Sciences* 2011; **6**(15): 3771-3777.

[23] Twfek KG, Mansour EA. **Theoretical and Experimental Analysis of the Wind Turbine Performance**. *Tikrit Journal of Engineering Sciences* 2020; **27**(4): 114-120.

[24] Wali SA, Muhammed AA. **Power Sharing and Frequency Control in Inverter-Based Microgrids**. *Tikrit Journal of Engineering Sciences* 2022; **29**(3): 70-81.

[25] Hilme I, Abdulkafi AA. **Energy-Efficient Massive MIMO Network**. *Tikrit Journal of Engineering Sciences* 2023; **30**(3): 1–8.

[26] Gaeid KS, Al Smadi T, Abubakar U. **Double Control Strategy of the PMSM Rotor Speed-Based Traction Drive Using a Resolver**. *Results in Control and Optimization* 2023; **13**: 100301.

[27] Ayyad S, Bani Baker M, Handam A, Al-Smadi T. **Reducing Highway Network Energy Bills Using Renewable Energy Systems**. *Civil Engineering Journal* 2023; **9**(11): 2914–2926.

[28] Khaldoon AO, kamil NY, Abbas AA, Al Smadi T. **A Novel Flying Robot Swarm Formation Technique Based on Adaptive Wireless Communication Using a MUSIC Algorithm**. *International Journal of Electrical and Electronics Research* 2024; **12**(2): 688–695.

[29] Dash L, Pattanayak BK, Laha SR, Pattnaik S, Mohanty B, Habboush AK, Al Smadi T. **Energy-Efficient Localization Technique Using Multilateration for the Reduction of Spatially and Temporally Correlated Data in RFID**

System. *Tikrit Journal of Engineering Sciences* 2024; **31**(1): 101–112.

[30] Gaeid KS, Al Smadi T, Abubakar U. **Double Control Strategy of the PMSM Rotor Speed-Based Traction Drive Using a Resolver**. *Results in Control and Optimization* 2023; **13**: 100301.

[31] Laha SR, Pattanayak BK, Pattnaik S, Mishra D, Nayak DSK, Dash BB. **An IOT-Based Soil Moisture Management System for Precision Agriculture: Real-Time Monitoring and Automated Irrigation Control**. *2023 4th International Conference on Smart Electronics and Communication (ICOSEC)*; IEEE; 2023. pp. 451-455.

[32] Guo Q, He Z, Wang Z. **Predicting the Daily PM2.5 Concentration Employing Wavelet Artificial Neural Networks Based on Meteorological Elements in Shanghai, China**. *Toxics* 2023; **11**(1): 51.

[33] Laha SR, Pattanayak BK, Kumar S, Ray M, Pattnaik S. **IoT-Enabled Machine Learning for Comprehensive Water Quality Assessment in the Mahanadi River: A Multibelt Analysis of Seasonal Contamination and Predictive Modeling**. *Journal of Engineering* 2025; **2025**(1): 5549990.

[34] Guo Q, He Z, Wang Z. **Prediction of Hourly PM2.5 and PM10 Concentrations in Chongqing City in China Based on Artificial Neural Network**. *Aerosol and Air Quality Research* 2023; **23**(6): 220448.

[35] Mahapatra SK, Pattanayak BK, Pati B, Laha SR, Pattnaik S, Mohanty B. **An IoT Based Novel Hybrid-Gamified Educational Approach to Enhance Student's Learning Ability**. *International Journal of Intelligent Systems and Applications in Engineering* 2023; **11**(3): 374-393.

[36] Laha SR, Pattnaik S, Mahapatra SK, Pattanayak BK. **A Novel Hybrid Smart Appliances Control Framework for Specially Challenged Persons**. *Smart Sensors for Industry 4.0: Fundamentals, Fabrication and IIoT Applications*; 2025. pp. 57-69.

[37] Elzaghmouri BM, Habboush AK, Abu-Zanona M, Laha SR, Pattanayak BK, Pattnaik S, Mohanty B. **Securing Industrial IoT Environments through Machine Learning-Based Anomaly Detection in the Age of Pervasive Connectivity**. *International Journal of Intelligent Systems and Applications in Engineering* 2023; **12**(2): 733–740.

[38] Laha SR, Pattanayak BK, Pattnaik S. **Advancement of Environmental Monitoring System Using IoT and Sensor: A Comprehensive Analysis**. *AIMS Environmental Science* 2022; **9**(6): 771-800.

[39] Guo Q, He Z, Wang Z. **Assessing the Effectiveness of Long Short-Term Memory and Artificial Neural Network in Predicting Daily Ozone Concentrations in Liaocheng City**. *Scientific Reports* 2025; **15**(1): 6798.

[40] He Z, Guo Q, Wang Z, Li X. **A Hybrid Wavelet-Based Deep Learning Model for the Accurate Prediction of Daily Surface PM2.5 Concentrations in Guangzhou**. *Environmental Science and Pollution Research* 2025; **32**(5): 7890-7905.

[41] Abbas AK, Ayop R, Tan CW, Al Mashhadany Y, Takialddin AS. **Advanced Energy-Management and Sizing Techniques for Renewable Microgrids with Electric-Vehicle Integration: A Review**. *Results in Engineering* 2025; **20**: 106252.